v. 1, n. 9, 2021

International Journal of Health Science

SELF-REGULATION IN ELECTROENCEPHALOGRAPHIC SIGNALS DURING AN ARITHMETIC PERFORMANCE TEST: AN APPROACH WITH AN RMS FLUCTUATION FUNCTION

Florêncio Mendes Oliveira Filho
Senai Cimatec University Center
Bahia, Brazil
http://lattes.cnpq.br/4658060085712228
ORCID: 0000-0002-8675-6444

Gilney Figueira Zebende
State University of Feira de Santana
Bahia, Brazil
http://lattes.cnpq.br/2464685002862801
ORCID: 0000-0003-2420-9805

Everaldo Freitas Guedes
Federal University of Recôncavo Baiano,
Cruz das Almas, Bahia, Brazil
Brazilian Hospital Services Company
Climério de Oliveira Maternity Hospital,
Health Regulation and Evaluation Sector
Salvador, Bahia, Brazil
http://lattes.cnpq.br/5223749020009535
ORCID: 0000-0002-2986-7367

Aloísio Machado da Silva Filho
State University of Feira de Santana
Bahia, Brazil
http://lattes.cnpq.br/0550981915615186
ORCID: 0000-0001-8250-1527

Arleys Pereira Nunes de Castro
Rui Barbosa University Center
Bahia, Brazil
http://lattes.cnpq.br/8491354585378127
ORCID: 0000-0001-8221-4843

Juan Alberto Leyva Cruz
State University of Feira de Santana
Bahia, Brazil
http://lattes.cnpq.br/1173503191220599
ORCID: 0000-0003-4019-4463

Abstract: The state of functioning of the brain by self-regulation techniques allows the user to train the corresponding brain functions by different methods, making it possible to condition the brain to balance its functioning and im- prove memory, concentration and confidence. In this study, we investigated 5 individuals based on self-regulation of learning generated by responses to basic arithmetic stimuli, subtraction of two numbers. To do this, we study 5 of active EGG channels during arithmetic tests. For the series generated by the test, we applied the DFA method to assess the autocorrelation of the series, here representing the areas: frontal, central and parietal in two mo- ments of the scales, $n \leq 60$ and $n > 60$ (30 seconds). We also investigate the rms root mean square function at three moments of the scale, $n < 10$ (5 seconds), $10 < n < 100$ and $n > 100$ (50 seconds). The results found revealed non-stationary behavior with Brownian noise transition for $n\ 60 \geq$ and persistence for $n > 60$. With the rms root mean square function, on average, we verified that the central region, when compared to the other re- gions, the results revealed a positive difference for the fluctuation amplitude, with the exception of $Cz(2) - Af_4(9)$ em $n > 100$. Our findings pointed out that modeling DFA and rms function was useful for investigating responses to brain stimuli. Our research is a contribution to EEG analysis and to the areas of biophysics, systems analysis and digital signal processing.
Keywords: Self-regulation, Time series, EEG, Cognitive stimuli, rms function

INTRODUÇÃO

Self-regulation methods allow the user to train the corresponding brain functions through Brain Mapping techniques, such as electroencephalography (EEG) [1, 2]. Among

these methods, conditioning modalities, in addition to reestablishing electrophysiological patterns, such as neurofeedback, train the brain to balance its functioning and improve its memory, concentration and confidence [3]. This type of approach has attracted the interest of researchers from different areas of knowledge such as biophysics, systems analysis and signal processing. [4–10].

From the use of traditional spectral analysis approaches, such as the Fourier, Hilbert and Wavelet transforms, recent studies have demonstrated the approach of techniques related to the intentional control of cognitive stimuli [11–14] . It is possible to cite the work of Keyman (2019)[5] who studied the management of stress, directed to deeply located limbic areas. Young (2019) [15] research that evaluated psychiatric disorders associated with emotion regulation in soldiers during combat training. Young (2017)[16] studied positive stimuli, including autobiographical memories, and also examined the therapeutic effectiveness of real-time functional training. Bir- baumer (2009)[17] and Stoechel (2014)[18] stated that using the neurofeed- back/neuroimaging technique can be used to assess and/or alter patterns of brain activity associated with cognition or behavior while an individual is inside the real-time magmatic resonance scanner.

With a look at temporal coherence, which are brain areas correlated to the same scale, this study aims to analyze: i) the self-affinity of scales of EEG channels selected through the method of Rectified Fluctuation Analysis (DFA) [19]; ii) the fluctuation amplitude of a correlated signal pair generated by two active channels through the difference of the fluctuation amplitude

[1]. To present these findings, this paper has been divided into methodology and data (Section 2), results (Section 3) and conclusions (Section 4).

METODOLOGIA AND DATA

THE DATA

The database used in this research is in the public domain and is available at: *https* : *//physionet.org/content/eegmat/*1.0.0/. This database contains EEG recordings of subjects who performed arithmetic tasks at two times, before and during. EEGs were recorded using the Neurocom EEG system of 23 channels (Ukraine, XAI-MEDICA)[3, 20].

The arithmetic task consisted of serial subtraction of two numbers. Each test started with the communication numbers of 4 digits (mining) and 2 digits (subtracting), for example: 3141 and 42. The EEG data files were made available in European Data Format (.EDF), so each test has 2 files:

1. with the suffix ”1” - the background EEG recording of a subject (before the mental arithmetic task);
2. with suffix ”2” - EEG recording during the mental arithmetic task.

According to Zyma et al. (2019)[3], during the EEG recording, the par- ticipants sat in a soundproof darkroom, comfortably reclining in an armchair. Before the experiment, participants were instructed to try to relax during the resting state and informed about the arithmetic task. The same participants were also asked to mentally count without speaking or using finger move- ments, accurately and quickly, at the pace they had set. After 3 minutes of adaptation to the experimental conditions, the resting state EEG recording was made with eyes closed (in the next 3 minutes). Then, the participants performed a mental arithmetic task - serial subtraction - for 4 minutes.

At the end, the participants were divided into two groups: i) Group ”A” (24 subjects) with good quality counting (average number of operations per 4 minutes = 21) and ii) Group ”B” (12 subjects) with poor quality count (average number of operations per 4 minutes = 7).

In the present study, we explore the time series of 5 active EEG channels located in the regions: a) frontal - $Af_3(7)$ and $Af_4(9)$, b) central - $Cz(2)$ and c) parietal - $P\ 3(16)$ and $P\ 4(18)$. The figures 1 and 2 denote the raw series. The files chosen in the database were: *S*01-*S*02-*S*03-*S*04 -*S*05.

DETRENDE FLUCTUATIONS ANALYSIS

Peng *et al.* (1994)[19] developed the DFA to analyze the existence of serial dependence, with the advantage of being also possible to be used in non-stationary data. Its main advantage is to avoid spurious detection of long-range dependence due to nonstationary data. For a given $u\ (i)$ signal, the algorithm is described as follows:

Consider a correlated signal time series of $u(i)$ (EEG signal), where $i = 1, \cdots, N$, where N is the total number of points in the time series. We integrate the sign $u(i)$ and get $y(k) = \Sigma^{k}_{i=1}$ $[u(i) - <u>]$, where $<u>$ is the mean of $u(i)$.

The integrated signal $y(k)$ is boxed (no overlapping) of the same size n (timescale). For each box of size n, we fit $y_n(k)$ on each box using a first-order linear regression, which represents the trend in the box. Every process is obtained by the method of least squares. The integrated series $y(k)$ is subtracted from the adjusted series $y_n(k)$ in each size n of the box. Afterwards, for each box of size n, the root mean square will be calculated, that is,

$$F_{DFA}(n) = \sqrt{\frac{1}{N_{max}} \sum_{k=1}^{N_{max}} [y(k) - y_n(k)]^2}; \qquad (1)$$

The calculation is repeated for a wide range of scales, ie, $4 \leq n \leq N/4$. Next, it is verified that the function F_{DFA} characterizes a power law of the type $F_{DFA} \sim n^{\alpha}DFA$, where α_{DFA} will be the long-range correlation indicator.

The interpretation of the relationship is given as follows: $\alpha_{DFA} < 0.5$ (anti-persistent signal), $\alpha_{DFA} = 0.5$ (non-correlated white noise), $\alpha_{DFA} > 0.5$ (persistent signal - long range correlation), α_{DFA} ‘ 1, (1/*f* noise), $\alpha_{DFA} >$ 1 (non-stationary) and α_{DFA} ‘ 3/2 (Brownian noise).

At this stage, the DFA method allows detection of long-range correlations embedded in apparently non-stationary time series and also avoids spurious detection of apparent long-range correlations, which are an artifact of non- stationarity [21–24].

RMS FLOAT FUNCTION

The root mean square fluctuation function (*rms*) appears with the in- tention of measuring the fluctuation difference between two EEG channels. This function is an increment given to the DFA method and proved to be very useful in the application of electrophysiological signals, as it is possible to study how much two regions of the brain are associated to the same scale (temporal coherence) [1, 2, 24].

The procedure adopted in this research consists of calculating the DFA of two time series individually and then subtracting the results (see equation 2).

$$\Delta logF_{Cz(2):xx} = \Delta logF_{DFACz(2} - \Delta logF_{DFA-xx} \quad (2)$$

From the function $\Delta logF_{Cz(2):xx}$ we can infer that the amplitude of the fluctuation relative to *rms* can be seen by three conditions:

- If $\Delta logF_{Cz(2):xx} > 0$, then the amplitude of the fluctuation function *rms* around channel $Cz(2)$ with respect to channel xx is greater;
- If $\Delta logF_{Cz(2):xx} = 0$, then the amplitude of the fluctuation function *rms* around channel $Cz(2)$ with respect to channel xx is zero;
- If $\Delta logF_{Cz(2):xx} < 0$, then the amplitude of the fluctuation function *rms* around channel $Cz(2)$ with respect to channel xx is smaller.

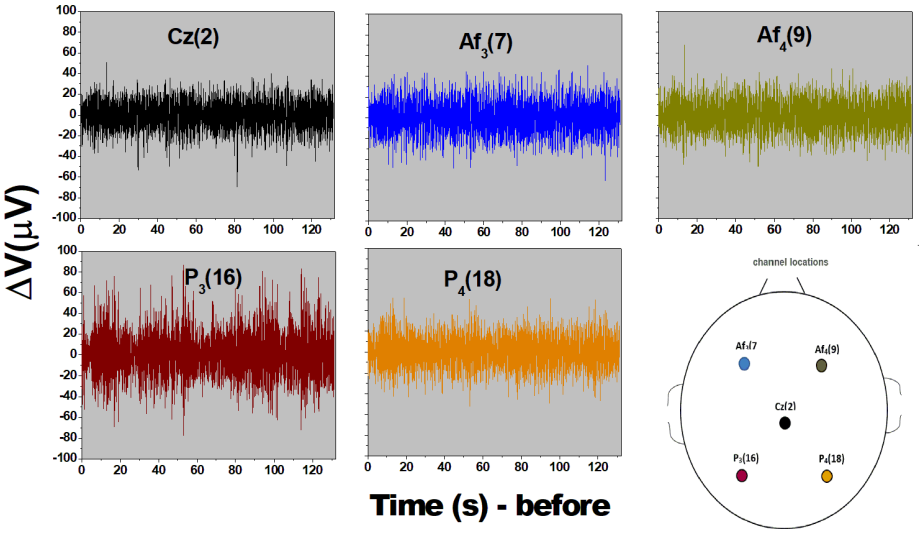

Figure 1: Original EEG signal series. Channels $Af_3(7)$, $Af_4(9)$ located in the right/left frontal polar region of the brain, $Cz(2)$ located in the central region and $P\,3(16)$ and $P\,4(18)$ located in the right/left parietal polar region of the brain. <*url:https://physionet.org/content/eegmat/*1.0.0/>.

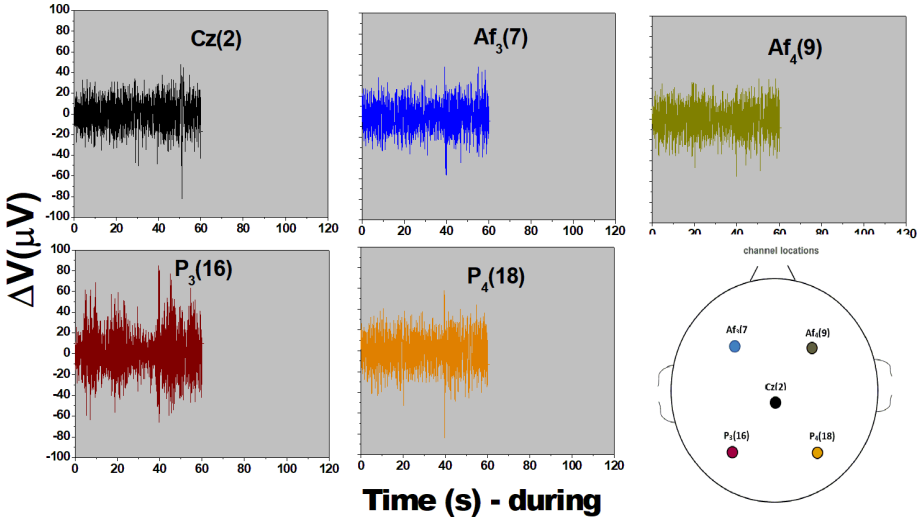

Figure 2: Original EEG signal series. Channels $A_3f\,(7)$, $Af_4(9)$ located in the right/left frontal polar region of the brain, $Cz(2)$ located in the central region and $P\,3(16)$ and$P\,4(18)$ located in the right/left parietal polar region of the brain. <*url:https://physionet.org/content/eegmat/*1.0.0/>.

RESULTS

In this investigation, time series were extracted with the following crite- ria: i) before (65.536 points - 131.068 seconds) and ii) during (30.515 points - 61.026 seconds) of the arithmetic activity. Both series were generated at a machine rate of 0.002 ms. 5 EEG channels were selected, represented by 5 ac- tive subjects. For analysis of the chosen channels, $Af_3(7)$ and $Af_4(9)$, frontal region, $Cz(2)$, brain midpoint and P 3(16) and P 4(18), region parietal, we calculated the DFA before and during the arithmetic test, here represented by the figures ref fig: dfaantes and ref fig: dfaduring.

For each channel (previous task), we calculate α_{DFA} for two moments, $n \leq 60$ and $n > 60$ (30 seconds). The choice in the neighborhood of n refers to a change in behavior on the curve. At first, n ≤ 60 all channels presented α_{DFA} above 1.0, while for $n > 60$, the channels presented α_{DFA} between 0.62 and 0.93, with emphasis on $Af_3(7)$ of subjects $S04$ and $S05$, both with α_{DFA} greater than 1.0 ($\alpha_{DFA}S04 = 1.12$ and $\alpha_{DFA}S05 = 1.01$). (See table 1).

For each channel (during task), we also calculate α_{DFA} for two moments, $n \leq 60$ and $n > 60$. At first, $n \leq 60$ all channels showed $alpha_{DFA}$ above 1.0, while for $n > 60$, the channels showed $alpha_{DFA}$ between 0.56 and 0.99, with emphasis on $Af_3(7)$ and P 3(16) of subjects $S02$, $Cz(2)$ and $Af_3(7)$ of subjects $S04$, $Cz(2)$ and $Af_3(7)$ of the subject $S05$. $\alpha_{DFA}(S02) = 1.04$ and 1.23, $\alpha_{DFA}(S04) = 1.10$ and $\alpha_{DFA}(S05) = 1.43$ and 1.02 (see table 1).

Then, the mean values α_{DFA} (task before / during task) were calculated for $n \leq 60$ and $n > 60$. For before and during, n ≤ 60, all channels had $\alpha_{DFA} > 1.0$, only channel $Cz(2)$ (during), $n > 60$, had $\alpha_{DFA} > 1.0$ (1.06) (See table 2).

For the purpose of temporal coherence, we analyze, through the function $\Delta logF_{DFA}$, equation ref 2, the effect of the amplitude of the fluctuation based on the channel $Cz(2)$. See the figures ref fig: deltadfaantes, ref fig: deltadfaantes. To visualize these differences, we look at the scales of n, de- fined here as $n <$ 10 (5 seconds), $10 < n < 100$, and $n > 100$ (50 seconds).

For the purpose of temporal coherence, we analyze, through the function $DeltalogF_{DFA}$, equation ref 2, the effect of the amplitude of the fluctuation based on the channel $Cz(2)$. See the figures 5, 6.

In the task during the task, figure ref fig: graph5: in $S01$ $Cz(2) - Af_4(9)$ for $n > 100$ presented negative difference, $S02$ for $Cz(2) - P_4(18)$ showed negative difference for all scales, $S03$ for n $Cz(2) - Af_4(9)$ showed negative difference. $S04$ and $S05$ in $n > 100$, $Cz(2)$ $P_4(16)$ showed a negative difference.

In the task during the task, figure ref fig: graph6: at $S01$ for $n > 100$, $Cz(2) - Af_3(7)$ and $Cz(2) - Af_4(9)$ revealed negative difference, in $S02$ $Cz(2) - P$ 3(16), revealed negative difference, $S03$ for $n > 100$, $Cz(2) - Af_4(9)$, showed negative difference, $S04$ for $n < 100$, negative difference for $Cz(2) - Af_4(18)$ and for $n > 100$, $Cz(2) - Af_4(9)$ showed negative difference and in $S05$ for $n < 100$, $Cz(2) - P_4(18)$ revealed negative difference.

Observations were also made about the average difference of the chan- nels $Af_3(7)$, $Af_4(9)$, P 3(16) and P 4(18) in relation to $Cz(2)$, figure ref fig: graph7. For the previous task, on average, the difference in the fluc- tuation amplitude was positive. With an abbreviated negative difference to $Cz(2)$ P 3(16), on large scales $n > 100$. As for the later task, the difference of the channel $Cz(2)$ in relation to the others, through the root mean square fluctuation function (*rms*), showed a positive difference with the exception of $Cz(2) - Af_4(9)$ which revealed a negative difference for $n >$ 100.

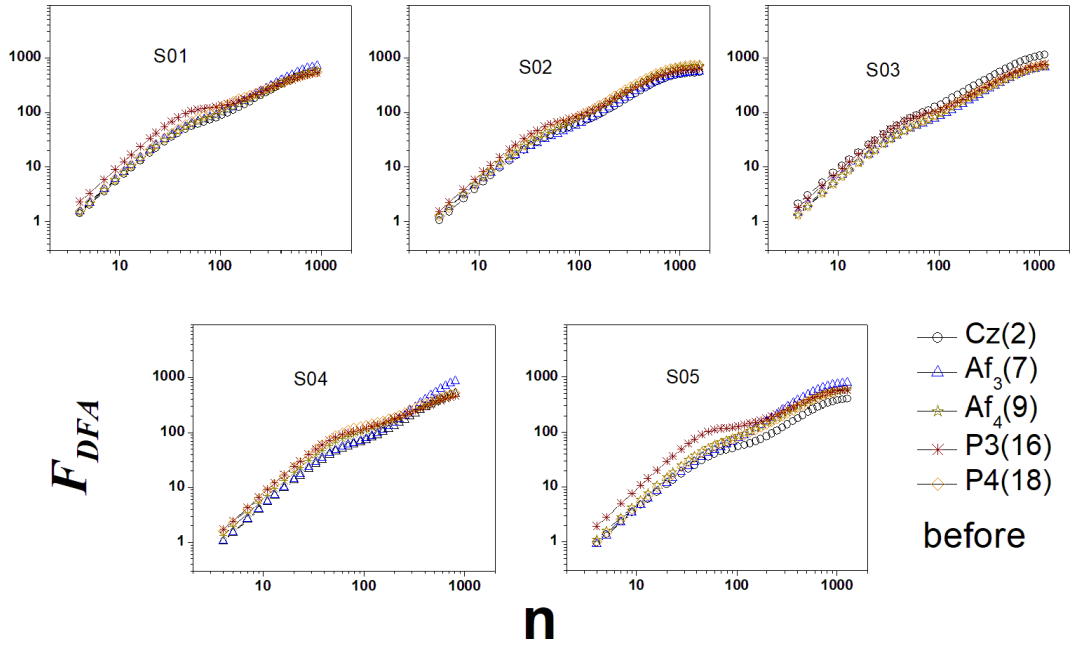

Figure 3: 001, 002, 003, 004 and 005 denote the research subjects.

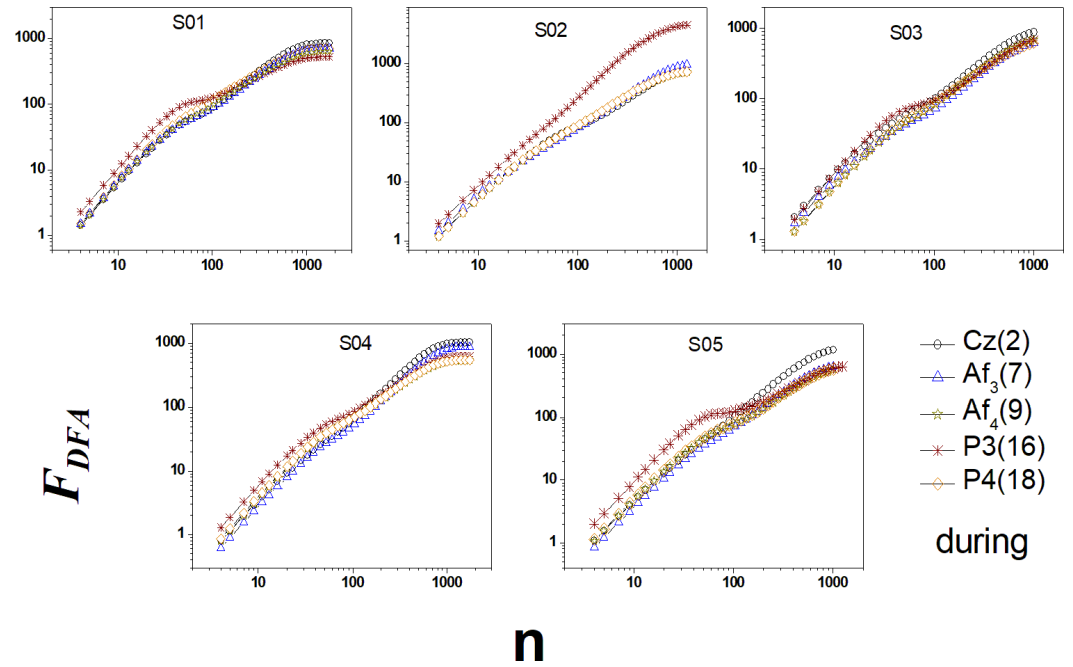

Figure 4: 001, 002, 003, 004 and 005 denote the research subjects.

		α_{DFA} (**before**)		α_{DFA} (**during**)	
Subjects	**Channels**	$n \leq 60$	$n > 60$	$n \leq 60$	$n > 60$
	Cz(2)	1.47	0.89	1.43	0.88
	Af_3(7)	1.42	0.93	1.38	0.81
S01	**Af_4(9)**	1.42	0.84	1.43	0.73
	P3(16)	1.48	0.66	1.47	0.56
	P4(18)	1.45	0.72	1.45	0.70
	Cz(2)	1.42	0.85	1.42	0.90
	Af_3(7)	1.26	0.87	1.28	1.04
S02	**Af_4(9)**	1.37	0.88	1.40	0.90
	P3(16)	1.42	0.78	1.40	1.23
	P4(18)	1.41	0.86	1.42	0.89
	Cz(2)	1.38	0.92	1.27	0.99
	Af_3(7)	1.36	0.91	1.23	0.98
S03	**Af_4(9)**	1.41	0.89	1.38	0.98
	P3(16)	1.45	0.84	1.40	0.87
	P4(18)	1.43	0.87	1.41	0.88
	Cz(2)	1.49	0.95	1.40	1.10
	Af_3(7)	1.51	1.12	1.47	1.10
S04	**Af_4(9)**	1.52	0.71	1.52	0.81
	P3(16)	1.51	0.64	1.44	0.78
	P4(18)	1.56	0.65	1.49	0.82
	Cz(2)	1.38	0.85	1.26	1.43
	Af_3(7)	1.48	1.01	1.46	1.02
S05	**Af_4(9)**	1.46	0.82	1.45	0.90
	P3(16)	1.54	0.62	1.53	0.67
	P4(18)	1.51	0.88	1.45	0.89

Table 1: Values of $\alpha_{DF\ A}$ for both moments (Before / During). Represented by $\alpha_{DF\ A}$ for n 60 and n >60 associated with channels $Af_3(7)$, $Af_4(9)$, $Cz(2)$, P 3(16) and P 4(18). Subjects: 001, 002, 003, 004 and 005. n=60 corresponds to 30 seconds.

		α_{DFA} (**before**)		α_{DFA} (**during**)	
	Channels	n ≤ 60	n > 60	n ≤ 60	n > 60
	Cz(2)	1.43	0.89	1.36	1.06
	Af_3(7)	1.41	0.97	1.36	0.99
Mean	**Af_4(9)**	1.44	0.83	1.44	0.86
	P3(16)	1.48	0.71	1.45	0.82
	P4(18)	1.47	0.80	1.44	0.84

Table 2: Average values of $\alpha_{DF\ A}$. n = 60 corresponds to 30 seconds.

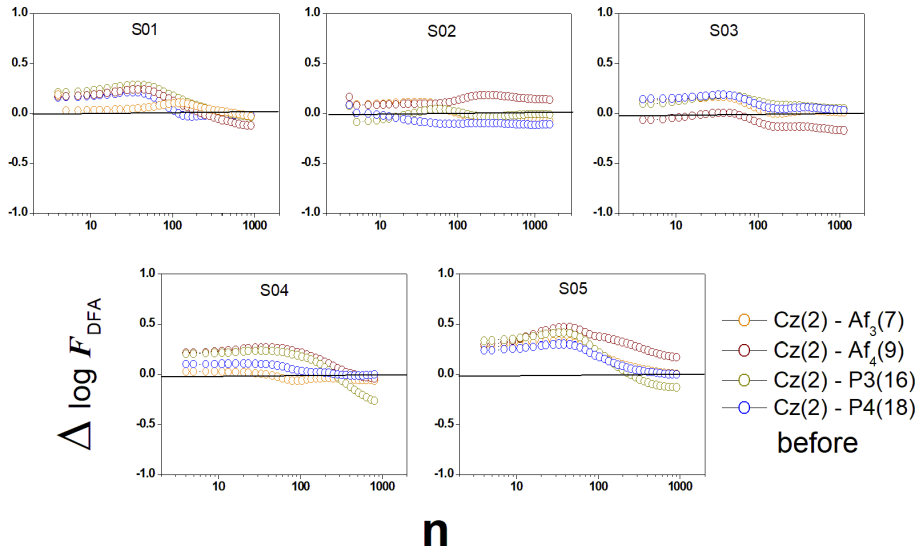

Figure 5: Difference in amplitude of fluctuation between channels via $\Delta logF_{DF\,A}$ function for task before.

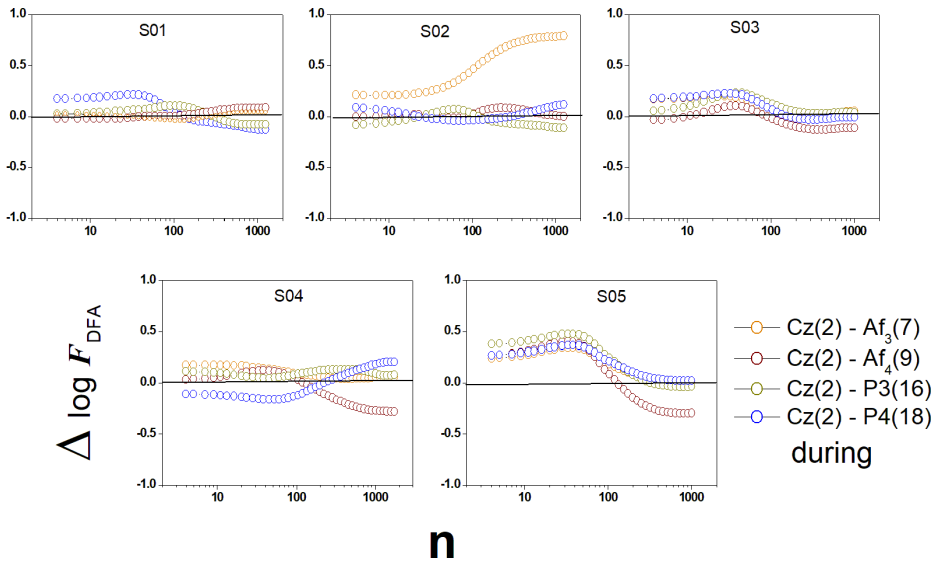

Figure 6: Difference in amplitude of fluctuation between channels via $\Delta logF_{DF\,A}$ function for task during.

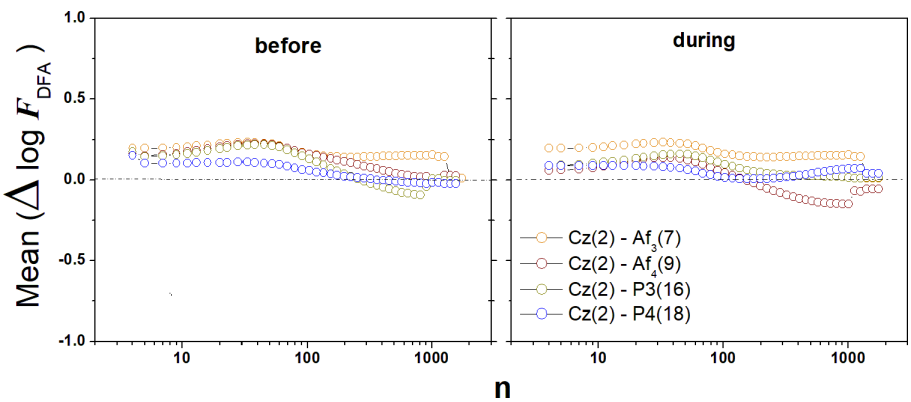

Figure 7: Curves generated for before and during. Average value.

CONCLUSION

We studied the behavior of EEG signals in 5 individuals who perform arithmetic tasks at two moments, before and during, from the time series of 5 active EEG channels located in the regions: frontal - $Af_3(7)$ and $Af_4(9)$, central - $Cz(2)$ and parietal - $P\ 3(16)$ and $P\ 4(18)$ of the brain.

Initially, we investigate the autocorrelation exponent α_{DFA} for two scale values, $n \leq 60$ and $n > 60$. For $n \leq 60$, we find $\alpha_{DFA} > 1.0$, character- istic behavior of non-stationarity with transition to Brownian noise. While for $n > 60$, we find α_{DFA} varying between 0.62 and 0.93, that is, persistent signal (long-range correlation).

Furthermore, we investigated the influence of the $Cz(2)$ channel, located in the central region of the brain. We look at the before, during and also at the average. On average, we found that the central region, when compared to the others, frontal ($Af_3(7)$ - $Af_4(9)$) and parietal ($P\ 3(16)$ - $P\ 4(18)$), through of the root mean square fluctuation function (*rms*), showed a pos- itive difference for the amplitude of the fluctuation, with the exception of $Cz(2)$ $Af_4(9)$, which showed a negative difference for $n > 100$. In terms of temporal coherence, for arithmetic activity, the central region, represented by the channel $Cz(2)$, became more active when compared to the other re- gions.

We understand that approaches taken in this line are relevant, and that, above all, it can contribute to the aspect that brain coherence is not only seen in the frequency domain (Hz), but also in time through self-related processes.

AGRADECIMENTOS

Florêncio Mendes Oliveira Filho thanks the group Modeling in Complex Systems.

REFERENCES

1. G. F. Zebende, F. M. Oliveira Filho, J. A. L. Cruz, Auto-correlation in the motor/imaginary human eeg signals: A vision about the fdfa fluctuations, PloS one 12 (9) (2017).

2. F. Oliveira Filho, J. L. Cruz, G. Zebende, Analysis of the eeg bio-signals during the reading task by dfa method, Physica A: Statistical Mechanics and its Applications 525 (2019) 664–671.

3. I. Zyma, S. Tukaev, I. Seleznov, K. Kiyono, A. Popov, M. Chernykh,
O. Shpenkov, Electroencephalograms during mental arithmetic task per- formance, Data 4 (1) (2019) 14.

4. R. A. Kulka, W. E. Schlenger, J. A. Fairbank, R. L. Hough, B. K. Jordan, C. R. Marmar, D. S. Weiss, Trauma and the Vietnam war gen- eration: Report of findings from the National Vietnam Veterans Read- justment Study., Brunner/Mazel, 1990.

5. J. N. Keynan, A. Cohen, G. Jackont, N. Green, N. Goldway, A. Davi- dov, Y. Meir-Hasson, G. Raz, N. Intrator, E. Fruchter, et al., Electrical fingerprint of the amygdala guides neurofeedback training for stress re- silience, Nature human behaviour 3 (1) (2019) 63–73.

6. S. J. Banks, K. T. Eddy, M. Angstadt, P. J. Nathan, K. L. Phan, Amygdala–frontal connectivity during emotion regulation, Social cog- nitive and affective neuroscience 2 (4) (2007) 303–312.

7. S. E. Bruce, K. R. Buchholz, W. J. Brown, L. Yan, A. Durbin, Y. I. Sheline, Altered emotional interference processing in the amygdala and insula in women with post-traumatic stress disorder, NeuroImage: Clin- ical 2 (2013) 43–49.

8. A. Doll, B. K. Ho¨lzel, S. M. Bratec, C. C. Boucard, X. Xie, A. M. Wohlschl¨ager, C. Sorg, Mindful attention to breath regulates emotions via increased amygdala–prefrontal cortex connectivity, Neuroimage 134 (2016) 305–313.

9. P. G. Gasquoine, Contributions of the insula to cognition and emotion, Neuropsychology review 24 (2) (2014) 77–87.

10. Y. Koush, D.-E. Meskaldji, S. Pichon, G. Rey, S. W. Rieger, D. E. Linden, D. Van De Ville, P. Vuilleumier, F. Scharnowski, Learning con- trol over emotion networks through connectivity-based neurofeedback, Cerebral cortex 27 (2) (2017) 1193–1202.

11. M. Soleymani, M. Pantic, T. Pun, Multimodal emotion recognition in re- sponse to videos, IEEE transactions on affective computing 3 (2) (2011) 211–223.

12. J. Kortelainen, E. V¨ayrynen, T. Sepp¨anen, High-frequency electroen- cephalographic activity in left temporal area is associated with pleasant emotion induced by video clips, Computational intelligence and neuro- science 2015 (2015).

13. S. Weiss, H. M. Mueller, The contribution of eeg coherence to the inves- tigation of language, Brain and language 85 (2) (2003) 325–343.

14. A. A. Gonz´alez-Garrido, F. R. G´omez-Vel´azquez, R. A. Salido-Ruiz, A. Espinoza-Valdez, H. V´elez-P´erez, R. Romo-Vazquez, G. B. Gallardo- Moreno, V. D. Ruiz-Stovel, A. Mart´ınez-Ramos, G. Berumen, The anal- ysis of eeg coherence reflects middle childhood differences in mathemat- ical achievement, Brain and cognition 124 (2018) 57–63.

15. K. D. Young, Neurofeedback for soldiers, Nature human behaviour 3 (1) (2019) 16–17.

16. K. D. Young, G. J. Siegle, V. Zotev, R. Phillips, M. Misaki, H. Yuan, W. C. Drevets, J. Bodurka, Randomized clinical trial of real-time fmri amygdala neurofeedback for major depressive disorder: effects on symp- toms and autobiographical memory recall, American Journal of Psychi- atry 174 (8) (2017) 748–755.

17. N. Birbaumer, A. R. Murguialday, C. Weber, P. Montoya, Neurofeed- back and brain–computer interface: clinical applications, International review of neurobiology 86 (2009) 107–117.

18. L. E. Stoeckel, K. A. Garrison, S. S. Ghosh, P. Wighton, C. A. Han- lon, J. M. Gilman, S. Greer, N. B. Turk-Browne, M. T. deBettencourt, D. Scheinost, et al., Optimizing real time fmri neurofeedback for thera- peutic discovery and development, NeuroImage: Clinical 5 (2014) 245– 255.

19. C.-K. Peng, S. V. Buldyrev, S. Havlin, M. Simons, H. E. Stanley, A. L. Goldberger, Mosaic organization of dna nucleotides, Physical review e 49 (2) (1994) 1685.

20. A. L. Goldberger, L. A. Amaral, L. Glass, J. M. Hausdorff, P. C. Ivanov, R. G. Mark, J. E. Mietus, G. B. Moody, C.-K. Peng, H. E. Stanley, Phys- iobank, physiotoolkit, and physionet: components of a new research re- source for complex physiologic signals, circulation 101 (23) (2000) e215– e220.

21. J.-M. Lee, D.-J. Kim, I.-Y. Kim, K.-S. Park, S. I. Kim, Detrended fluc- tuation analysis of eeg in sleep apnea using mit/bih polysomnography data, Computers in biology and medicine 32 (1) (2002) 37–47.

22. J.-S. Lee, B.-H. Yang, J.-H. Lee, J.-H. Choi, I.-G. Choi, S.-B. Kim, Detrended fluctuation analysis of resting eeg in depressed outpatients and healthy controls, Clinical Neurophysiology 118 (11) (2007) 2489–2496.

23. R. Hardstone, S.-S. Poil, G. Schiavone, R. Jansen, V. V. Nikulin, H. D. Mansvelder, K. Linkenkaer-Hansen, Detrended fluctuation analysis: a scale-free view on neuronal oscillations, Frontiers in physiology 3 (2012) 450.

24. V. Barreto Mesquita, F. Mendes Oliveira Filho, P. C. Rodrigues, Detec- tion of crossover points in detrended fluctuation analysis: An application to EEG signals of patients with epilepsy, Bioinformatics (11 2020).